Diphenylethenyl- and methylphenylethenyl-substituted triphenylamines as effective hole transporting and emitting materials

M. Cekaviciute[a], J. Simokaitiene[a], G. Sych[a], J.V. Grazulevicius[a*], V. Jankauskas[b], D. Volyniuk[a], P. Stakhira[c], V. Cherpak[c], K. Ivanyuk[c]

[a] *Department of Polymer Chemistry and Technology, Kaunas University of Technology, Radvilenu pl. 19, LT-50254, Kaunas, Lithuania*

[b] *Department of Solid State Electronics, Vilnius University, Sauletekio al. 9, LT-10222, Vilnius, Lithuania*

[c] *Lviv Polytechnic National University, S. Bandera 12, 79013 Lviv, Ukraine*

**Corresponding author: juozas.grazulevicius@ktu.lt (Juozas V. Grazulevicius)*

Abstract

Diphenylethenyl- and methylphenylethenyl-substituted triphenylamines were prepared by condensation of trimethoxy-substituted triphenylamines with 2,2-diphenylacetaldehyde or 2-phenylpropionaldehyde respectively. The synthesized compounds were found to be capable of glass formation with glass transition temperatures above 49 ºC for methylphenylethenyl-substituted derivatives and above 82 ºC for diphenylethenyl-substituted compounds. The ionization potentials of the layers of the derivatives were found to be in the range of 5.31-5.44 eV. Time-of-flight hole drift mobility values of the glassy layer of tri(4-diphenylethenyl-2-methoxyphenyl)amine well exceeded 10^{-2} cm^2/Vs at high electric fields at room temperature. The clear dependence of the charge mobilities on the positions of methoxy groups was observed. Compounds having methoxy groups at the *meta* positions of triphenylamine groups exhibited superior hole-transporting

properties compared to the compounds having methoxy groups at the *ortho* positions. Blue-green emitting OLEDs based on triphenylamine derivatives exhibited relatively high efficiencies (brightness in order 10000 cd/m^2 and current efficiency from 4 to 10 cd/A) as for the fluorescent OLEDs.

Keywords: star-shaped triphenylamine derivatives, molecular glasses, hole drift mobility, organic light emitting diodes

1. INTRODUCTION

Derivatives of triphenylamine (TPA) represent one of the largest and one of the most widely studied classes of organic electroactive materials [1].They are successfully used in organic light-emitting diodes (OLEDs) for hole-transporting layers [2,3], as emitters [4] and as hosts of the triplet-emitting layers [5,6], in bulk-heterojunction [7,8] and dye-sensitized solar cells [9-11], electrophotographic photoreceptors [12,13], electrochromic devices [14,15], organic field-effect transistors (OFETs) [16,17]. The current level of development of OLEDs enables their effective application in the low-cost flat panel display technology and in lighting [18]. Improvement of the operation of OLEDs to a great extent depends on the increase of electroluminescence efficiency, in particular on the decrease of the power consumption while providing a high level of brightness. One possible way to achieve this task is the design and synthesizes of new organic multifunctional materials with excellent charge transporting and efficient emitting characteristics [19].

In this work we report on the synthesis and properties of star-shaped methoxy-substituted triphenylamine derivatives with diphenylethenyl or methylphenylethenyl groups. The later groups were introduced by the direct condensation of methoxy-substituted triphenylamines with appropriately substituted acetaldehydes in a similar way as reported earlier [20]. We also report on the fabrication and characterization of OLEDs based on the newly synthesized materials.

2. EXPERIMENTAL METHODS

2.1. Instrumentation

^{1}H NMR and ^{13}C NMR spectra were recorded with Varian Unity Inova [300 MHz (^{1}H), 75.4 MHz (^{13}C)] spectrometer at room temperature. All the data are given as chemical shifts δ (ppm) downfield from $Si(CH_3)_4$. Infrared (IR) spectra were recorded using PerkinElmer Spectrum GX II FT-IR System. The samples of the solid compounds were prepared in the form of KBr pellets. Mass spectra (MS) were obtained on a Waters ZQ. Elemental analysis was performed with an Exeter Analytical CE-440 Elemental. Differential scanning calorimetry (DSC) measurements were carried out in a nitrogen atmosphere with a TA Instruments Q10 calorimeter at a heating rate of 10 ºC/min. Thermogravimetric analysis (TGA) was performed on Mettler TGA/SDTA851e/LF/1100 in a nitrogen atmosphere at a heating rate of 20 ºC/min. Melting points were measured with Electrothermal MEL-TEMP melting point apparatus. Absorption spectra of dilute (10^{-5} M) solutions in tetrahydrofuran (THF) were recorded on a UV−vis−NIR spectrophotometer Lambda 950 (Perkin-Elmer). Fluorescence spectra, fluorescence quantum yields (Φ_F) and fluorescence transients of dilute solutions in THF (10^{-5} M) or solid films of the compounds were recorded with Edinburgh Instruments LS980 spectrometer. Cyclic voltammetry (CV) measurements were carried out using a micro-Autolab III (Metrohm Autolab) potentiostat-galvanostat equipped with a standard three-electrode configuration. A three-electrode cell equipped with a glassy carbon working electrode, an $Ag/AgNO_3$ (0.01 M in anhydrous acetonitrile) reference electrode and a Pt wire counter electrode were employed. The measurements were done in anhydrous dichloromethane with tetrabutylammonium hexafluorophosphate (0.1 M) as the supporting electrolyte under nitrogen atmosphere at a scan rate of 0.1 V/s [21-23].The measurements were calibrated using an internal standard, ferrocene/ferrocenium (Fc) system. The

oxidation potentials ($E_{1/2}$ vs Fc) for the reversible oxidation were taken as the average values of the anodic and cathodic peak potentials, Epa and Epc, respectively. Ionization potentials (I_P^{ep}) of the films of the synthesized compounds were measured by electron photoemission in air method as described before [24,25]. Hole drift mobilities were measured by a xerographic time of-flight (XTOF) method [12,26,27]. The layer thickness was in the range of 2.9-6.0 μm.

2.2. OLED fabrication

OLEDs were fabricated by means of vacuum deposition of organic semiconductor layers and metal electrodes onto pre-cleaned ITO coated glass substrate under vacuum of 10^{-5} Torr. The devices were fabricated by step-by-step deposition of the different organic layers. The layers of compounds **1** or **2** were used as hole-transporting and turquoise light-emitting layers. CuI was used as hole-injecting layer [28]. According to that the work function of CuI is lower than HOMO of **1** or **2** compounds; CuI hole-injecting layer completely reduced the energy barer between ITO and **1** or **2** compounds in fabricated OLEDs. Because of high hole mobility of **1** and **2** and their high LUMO levels (ca. -2 eV), 3,6-di(9-carbazolyl)-9-(2-ethylhexyl)carbazole (TCz1) [29] films were used as effective hole blocking and electron-transporting layers which promote charge balance in the light emitting layer and reduce the energy barrier of electron injection. TCz1 is a versatile compound [27,30,31]. It can be used as an effective electron-injection material, which helps to provide a stepwise electron transfer from the Ca:Al cathode to the emissive layer [29]. (8-Hydroxyquinoline) aluminum (Alq3) was used as electron-transporting and green light-emitting material. Ca layer topped with thick aluminum (Al) layer was used as the cathode.

The structures of the devices were as follows:

Device (A): ITO/CuI/**1**/TCz1/Ca:Al

Device (B): ITO/CuI/**1**/Alq3/Ca:Al

Device (C): ITO/CuI/**2**/TCz1/Ca:Al

Device (D): ITO/CuI/**2**/Alq3/Ca:Al

The active area of the obtained devices was 3x6 mm.

The density-voltage, luminance-voltage characteristics of OLEDs were measured using a semiconductor parameter analyzer (HP 4145A) in air without passivation immediately after fabrication of the devices. The measurements of brightness were done using a calibrated photodiode [32]. The electroluminescence spectra were recorded with an Ocean Optics USB2000 spectrometer.

2.3. Materials

All the required chemicals, i.e. 2,2-diphenylacetaldehyde, 2-phenylpropionaldehyde, (+/-)-camphor-10-sulfonic acid were obtained from Sigma-Aldrich and used as received. 2,2',2''-Trimethoxytriphenylamine (Mp = 144-147 ºC, lit. Mp = 139.5-140 ºC [33]) and 3,3',3''-trimethoxytriphenylamine were obtained under Ullmann conditions [34,35].

General procedure for the synthesis of compounds **1-4.** They were prepared by condensation of the appropriate o- or m- trimethoxy-substituted triphenylamine derivative (1 g, 2.98 mmol) with diphenylacetaldehyde (2.9 g, 14.8 mmol) or 2-phenylpropionaldehyde (2.0 g, 14.8 mmol) in toluene at a reflux temperature, in the presence of (+/-)-camphor-10-sulfonic acid (0.7 g, 3.0 mmol). The reaction mixtures were stirred at the reflux temperature for 24 h. The reactions were monitored by thin-layer chromatography (TLC). When the reactions were finished the solvent was distilled in vacuum and the crude product was subjected to purification by silica gel column chromatography.

Tris(4-diphenylethenyl-2-methoxyphenyl)amine (1) was prepared according to the general procedure from 2,2',2''-trimethoxytriphenylamine and 2,2-diphenylacetaldehyde. The resulting product was purified by column chromatography using the eluent mixture of acetone, dichloromethane and hexane in a volume ratio of 1:1:15. Yellow amorphous powder was obtained after precipitation in methanol with the yield of 1.04 g (40 %). IR ν_{max} (KBr): 3076, 3052, 3019 (C-H Ar), 2930 (C-H), 2829 (O-CH_3), 1589, 1505 (C=C Ar), 1279 (C-O-C). ^{1}H NMR (300 MHz,

$CDCl_3$) δ (ppm): 3.10 (s, 9H, -OCH_3), 6.36 (s, 3H, Ar), 6.54 (s, 6H, Ar), 6.92 (s, 3H, -C=CH), 7.21-7.32 (m, 30H, Ar). ^{13}C NMR (75.4 MHz, $CDCl_3$) δ (ppm): 55.00, 112.90, 122.68, 123.58, 127.31, 128.16, 128.68, 130.45, 132.96, 135.86, 140.89, 143.40, 151.90. Elemental analysis for $C_{63}H_{51}NO_3$: % calcd. C 86.97, H 5.91, N 1.61, O 5.52; % found C 86.39, H 6.16, N 1.73. MS (APCI+, 20V), m/z(%): 871 ($[M+H]^+$, 60).

Tri(4-diphenylethenyl-3-methoxyphenyl)amine (2) was prepared according to the general procedure from 3,3',3''-trimethoxytriphenylamine and 2,2-diphenylacetaldehyde. The resulting product was purified by column chromatography using the eluent mixture of THF and hexane in volume ratio of 1:20. Yellow crystals were obtained after recrystallization from methanol with the yield of 0.74 g (29 %). Mp = 201-204 ºC. IR ν_{max} (KBr): 3077, 3055, 3021 (C-H Ar), 2932 (C-H), 2832 (O-CH_3), 1593, 1494 (C=C Ar), 1224 (C-O-C). ^{1}H NMR (300 MHz, $CDCl_3$) δ (ppm): 3.65 (s, 9H, -OCH_3), 6.24 (d, 3H, *J* = 8.0 Hz, Ar), 6.51 (s, 3H, -C=CH), 6.56(d, 3H, *J* = 8.5 Hz, Ar), 7.10 (s, 3H, Ar), 7.18-7.31 (m, 30H, Ar). ^{13}C NMR (75.4 MHz, $CDCl_3$) δ (ppm): 55.73, 106.61, 116.63, 121.69, 122.78, 127.32, 128.00, 128.57, 130.82, 141.62, 144.09, 147.04, 158.55. Elemental analysis for $C_{63}H_{51}NO_3$: % calcd. C 86.97, H 5.91, N 1.61, O 5.52; % found C 86.11, H 5.88, N 1.79. MS (APCI+, 20V), m/z(%): 871($[M+H]^+$, 100).

Tri[4-(2-mehyl-2-phenylethenyl)-2-methoxyphenyl]amine (3) was prepared according to the general procedure from 2,2',2''-trimethoxytriphenylamine and 2-phenylpropionaldehyde. The resulting product was purified by column chromatography using the eluent mixture of acetone, dichloromethane and hexane in a volume ratio of 1:1:15. Yellowish amorphous powder was obtained after precipitation in methanol with the yield of 0.79 g (37 %). IR ν_{max} (KBr): 3078, 3053, 3024 (C-H Ar), 2954, 2930 (C-H), 2830 (O-CH_3), 1594, 1506 (C=C Ar), 1276 (C-O-C). ^{1}H NMR (300 MHz, $CDCl_3$) δ (ppm): 2.35-2.38 (m, 9H, -CH_3), 3.61-3.67 (m, 9H, -OCH_3), 6.83-6.87 (m, 3H, Ar), 6.92 (s, 3H, -C=CH), 6.94-6.96 (m, 3H, Ar), 7.32-7.35 (m, 3H, Ar), 7.36-7.44 (m, 9H, Ar), 7.52-7.58 (m, 6H, Ar). ^{13}C NMR (75.4 MHz, $CDCl_3$) δ (ppm): 18.09, 56.11, 113.94, 122.04, 124.35, 126.24, 127.20, 128.23, 128.55, 128.71, 134.35, 136.50, 144.67, 152.89. Elemental

analysis for $C_{48}H_{45}NO_3$: % calcd. C 84.30, H 6.63, N 2.05, O 7.02; % found C 84.53, H 6.72, N 2.01. MS (APCI+, 20V), m/z(%): 684 ($[M+H]^+$, 100).

Tri[4-(2-mehyl-2-phenylethenyl)-3-methoxyphenyl]amine (4) was prepared according to the general procedure from 3,3',3''-trimethoxytriphenylamine and 2-phenylpropionaldehyde. The resulting product was purified by column chromatography using the eluent mixture of THF and hexane in volume ratio of 1:50. Yellowish amorphous powder was obtained after precipitation in methanol with the yield of 0.24 g (12 %). IR ν_{max} (KBr): 3051, 3022 (C-H Ar), 2931 (C-H), 2832 (-O-CH_3), 1594, 1496 (C=C Ar), 1213 (C-O-C). ^{1}H NMR (300 MHz, $CDCl_3$) δ (ppm): 2.28-2.33 (m, 9H, -CH_3), 3.72-3.77 (m, 9H, -OCH_3), 6.68-6.78 (m, 3H, Ar), 6.80 (s, 3H, -C=CH), 6.97 (s, 3H, Ar), 7.31-7.34 (m, 3H, Ar), 7.36-7.44 (m, 9H, Ar), 7.58-7.63 (m, 6H, Ar). ^{13}C NMR (75.4 MHz, $CDCl_3$) δ (ppm): 17.89, 55.88, 107.00, 116.23, 122.36, 123.00, 126.28, 127.20, 128.49, 130.83, 136.53, 144.27, 147.55, 158.36. Elemental analysis for $C_{48}H_{45}NO_3$: % calcd. C 84.30, H 6.63, N 2.05, O 7.02; % found C 84.45, H 6.98, N 2.08. MS (APCI+, 20V), m/z(%): 684 ($[M+H]^+$, 100).

3. RESULTS AND DISCUSSION

3.1. Synthesis and characterization

The synthetic route towards the appropriate arylethenyl-substituted triphenylamines is shown in Scheme 1. Compounds **1–4** were prepared by one-step procedures from the appropriate trimethoxy-substituted triphenylamines by condensation with 2,2-diphenylacetaldehyde or 2-phenylpropionaldehyde in toluene at reflux temperature, in the presence of (+/-)-camphor-10-sulfonic acid. All the compounds were purified by column chromatography. They were identified by elemental analysis, IR-, ^{1}H NMR-, ^{13}C NMR- spectroscopies and mass spectrometry. The synthesized compounds were found to be soluble in common organic solvents such as THF, toluene, chloroform.

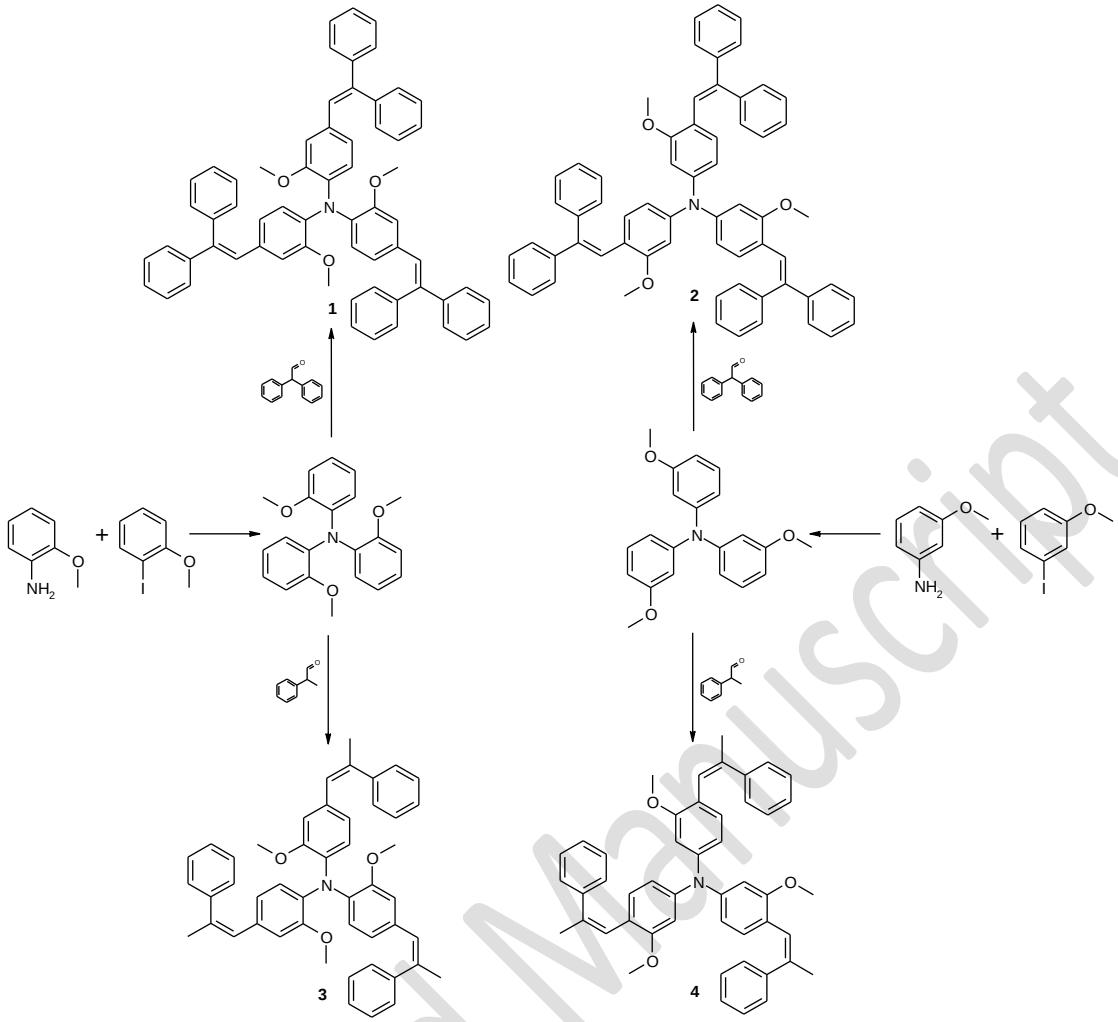

Scheme 1. Synthetic route of compounds **1**–**4**.

3.2. Thermal properties

The thermal characterization of the synthesized compounds was performed by DSC and TGA under a nitrogen atmosphere. The thermal characteristics are summarized in Table 1. The synthesized compounds (**1**–**4**) showed high thermal stability. The temperatures of the onsets of the thermal degradation (T_{dec}) were found to be lower for compounds **3**, **4** having methylphenylethenyl substituents (354 and 373 ºC respectively) than for compounds **1**, **2**, containing diphenylethenyl groups (418 and 439 ºC respectively). Compounds **1**, **3**, **4** were isolated after the synthesis as amorphous powders, while compound **2** was isolated as a crystalline substance. All the synthesized compounds (**1**–**4**) were found to be able to form molecular glasses. The glass transition

temperatures of diphenylethenyl-substituted triphenylamines (**1**, **2**) were found to be higher than those of the corresponding methylphenylethenyl-substituted derivatives (**3**, **4**). This observation can be explained by the larger conformation lability because of smaller substituents in the samples of compounds **3** and **4**.

<Table 1>

3.3. Optical and photophysical properties

Absorption and fluorescence spectra of the synthesized compounds are shown in Fig. 1. The absorption spectra of dilute solutions in THF of the derivatives are dominated by two absorption bands. The wavelengths of absorption maxima of the higher-energy bands (at ca 300 nm) were found to be close to that of triphenylamine [36]. The lower-energy absorption bands were similar in character and position. To evaluate these absorption bands density functional theory (DFT) calculations employing the B3LYP functional were performed for compounds **1**-**4**. The spectroscopic properties of the molecules were calculated using a time dependent density functional theory method (TDDFT), in conjunction with 6-31G(d,p) basis set with the Gaussian 09 program [37]. Absorption peaks witch appears in the range of 358-395 nm correspond to HOMO→LUMO and HOMO→LUMO+1 electronic transitions contributing to the $S_0 \rightarrow S_1$ and $S_0 \rightarrow S_2$ excitations. HOMO orbitals are localized on the triphenylamine core. LUMO and LUMO+1 orbitals are localized on two of arylethenyl sidearms with contribution from triphenylamine core. The absorption edges of diphenylethenyl-substituted compounds (**1**, **2**) were red shifted with respect of the absorption edges of the corresponding methylphenylethenyl-substituted derivatives (**3**, **4**) due to the increased conjugated systems [38]. The similar regularity was observed for the fluorescence spectra (Fig. 1). Fluorescence intensity maxima of diphenylethenyl-substituted compounds (**1**, **2**) exhibited bathochromic shifts with respect of the maxima of methylphenylethenyl-substituted

compounds (**3**, **4**). Moreover, fluorescence intensity maxima of *o*-methoxytriphenylamine-based derivatives (**1**, **3**) exhibited bathochromic shifts compared to those of *m*-methoxytriphenylamine-based derivatives (**2**, **4**). The emission spectra of the solid films of compounds **1**–**4** were found to be without vibronic features and were situated in between those of the dilute solutions in toluene (less polar) and in THF (more polar). The emission intensity maxima of the solutions of these four compounds in THF showed red-shifts with respect to those of the solutions in toluene. The solvatochromic effect was larger (ca. 24 nm) in the case of *ortho*-methoxy-substituted compounds **1** and **3**, compared with that observed for *meta*-methoxy-substituted compounds **2** and **4** (8-16 nm).

<Table 2>

<Figure 1>

Fluorescence quantum yields (Φ_F) of the dilute solutions in THF, toluene and of the solid films of compounds **1**–**4** are given in Table 2. The dilute solutions of *o*-methoxytriphenylamine-based derivatives **1** and **3** exhibited higher emission quantum yields than those of their *m*-methoxytriphenylamine-based counterparts **2** and **4**. Φ_F values observed for the dilute solutions of methylphenylethenyl-substituted compounds (**3, 4**) were found to be higher than those of diphenylethenyl-substituted compounds (**1, 2**). Φ_F values for the amorphous films of the synthesized compounds were found to be close and ranged from 2 to 3%. Fluorescence decay curves of the dilute solutions compounds **1**–**4** demonstrated mono-exponential decay profiles (Fig. 2). χ^2 values and weighted residuals were used as the goodness-of-fit criteria. Fluorescence life times (τ) of the dilute solutions of methylphenyl-substituted compounds (**3**, **4**) were found slightly longer than those of the corresponding diphenyl-substituted compounds (**1**, **2**).

<Figure 2>

3.4. Electrochemical, photoelectrical and charge transporting properties

Electrochemical properties of the synthesized compounds were studied by cyclic voltammetry (CV). The cyclic voltammograms of compounds **1**–**4** show the reversible oxidation steps with the peak height varying linearly with sweep rate and the same values of anodic and cathodic peak currents [39] (Fig. 3). The shapes of cyclic voltammograms were found to be similar for all the studied compounds. The electrochemical data are summarized in Table 3. The ionization potential values (I_p^{cv}) were determined from the values of the first oxidation potential with respect to ferrocene (Fc). The ionization potential values of the synthesized compounds were found to be very close and ranged from 4.88 to 4.94 eV. The electron affinities (EA^{cv}) were determined from the optical energy band gaps (E_g^{opt}) and ionization energy values. They ranged from -2.13 to -1.83 eV. The ionization potentials (I_p^{ep}) of the layers of compounds **1**–**4** were established by electron photoemission method in air (Fig. 4). The I_p^{ep} values of the compounds ranged from 5.31 to 5.44 eV. Both methods of estimation of ionization potentials revealed the same trend. The ionization potentials (I_p) values of the dilute solutions of methylphenyl-substituted compounds (**3**, **4**) were found slightly lower than those of the corresponding diphenyl-substituted compounds (**1**, **2**). I_p values of *o*-methoxytriphenylamine-based compounds (**1**, **3**) were found to be lower than those of *m*-methoxytriphenylamine-based compounds (**2**, **4**).

<Table 3>

<Figure 3>

<Figure 4>

Time of flight measurements were used for the estimation of charge-transporting properties of the synthesized compounds. Fig. 5 shows electric field dependencies of hole drift mobilities (μ) for the layers of compounds **1**–**4**. All the studied compounds showed linear dependencies of hole mobilities (μ) on the square root of the electric field. The hole-drift mobility values are summarized in Table 3. Diphenylethenyl-substituted compounds (**1**, **2**) showed higher charge mobilities than the corresponding methylphenylethenyl-substituted derivatives (**3**, **4**). Moreover, *meta*-methoxy-substituted compounds **2** and **4** exhibited higher charge mobilities than *ortho*-methoxy-substituted compounds **1** and **3**. The highest hole mobility was observed for the layer of compound **2**. It exceeded 10^{-2} cm^2/Vs at high electric fields.

<Figure 5>

3.5. Electroluminescent devices

Compounds **1** and **2** were tested in the structures of electroluminescent devices (OLEDs). Fig. 6 shows electroluminescence spectra of the OLEDs, the structures of which are described in the experimental part. The shapes of the electroluminescence spectra of the devices A and C are similar to those of fluorescence spectra of the solid films of **1** and **2**, respectively. Taking into account the values of HOMO and LUMO energy levels (Fig. 7 a), TCz1 was used as an electron-injection as well as hole blocking material in devices A and C. The devices B and D containing layers of Alq3 were characterized by broad emission bands with bathochromic shifts compared with the fluorescence spectra of vacuum deposited films of **1** and **2**. The electroluminescence of the devices B and D originate from the superposition of the emission bands **1** or **2** with those of Alq3. We assume that the electron−hole recombination takes place at the volume of the layers of **1** or **2** and Alq3 which provides excited states in these species under application of the external electric field.

<Figure 6>

<Figure 7>

It is evident from energy-band diagrams of the devices shown in Figure 7 that there are almost no energy barriers for injection of holes from CuI into HOMO level of **1** or **2**. The similar situation is observed for electron injection from Ca into the LUMO level of Alq3 or TCz1. Thus it can be assumed that effective double-carrier injection was possible. Characteristics of the devices A-D are shown in Figure 8. All the devices exhibited relatively high efficiencies as for the fluorescent OLEDs. High current efficiency of devices A and B is mainly due to excellent electron blocking properties of **1** and **2** as well as hole blocking properties of Alq3 [40] and TCz1. The recombination zone is located at the organic-organic interface, away from ITO and Ca contacts. In such a way, quenching of electroluminescence is reduced [41]. The turn-on voltages of devices B and D as well as of devices A and C are close due to similarity of their structures (Fig. 8 a). The turn-on voltages of the devices are low (ca. 3.0-3.5 V) showing the absence of energy barriers for both holes and electrons in the devices. The applied voltages were of the same order reaching of 15 V for all the devises (Fig. 8 a). The current density of device B was lower than that observed for the other devices (Fig. 8 a). This observation can be explained either by the difference in hole mobilities of compounds 1 (4.2×10^{-3} cm^2/Vs) and compound 2 (7.9×10^{-3} cm^2/Vs) or by the different balance of charges in the structure of device B.

<Figure 8>

Conclusions

We synthesized and characterized new derivatives of methoxytriphenylamine having diphenylethenyl or methylphenylethenyl moieties as substituents and studied their thermal, optical photophysical and photoelectrical properties. The synthesized triphenylamine derivatives were found to constitute glass-forming materials with glass transition temperatures being in the range of 49-102 °C as characterized by differential scanning calorimetry. Electron photoemission spectra of the amorphous films of the materials revealed ionization potentials of 5.25–5.55 eV. Time-of-flight hole mobilities in the solid amorphous layers of synthesized arylethenes reached 10^{-2} $cm^2/V \cdot s$ at high electric fields. All blue-green emitting OLEDs based on triphenylamine derivatives exhibited relatively high efficiencies (brightness in order 10000 cd/m^2 and current efficiency from 4 to 10 cd/A) as for the fluorescent OLEDs.

Acknowledgements

This work was supported by the Horizon 2020 ICT29-2014 project PHEBE (grant No 641725).

References

[1] Iwan A, Sek D. Polymers with triphenylamine units: photonic and electroactive materials. Prog Polym Sci 2011;36:1277–1325.

[2] Duan LA, Hou LD, Lee TW, Qiao JA, Zhang DQ, Dong GF, Wang LD, Qiu Y. Solution processable small molecules for organic light-emitting diodes. J Mater Chem 2010;20:6392–6407.

[3] Zhong CM, Duan CH, Huang F, Wu HB, Cao Y. Materials and devices toward fully solution processable organic light-emitting diodes. Chem Mater 2011;23:326–340.

[4] Zhang Q, Ning ZJ, Tian H. 'Click' synthesis of starburst triphenylamine as potential emitting material. Dyes Pigm 2009;81:80–84.

[5] Chaskar A, Chen HF, Wong KT. Bipolar host materials: a chemical approach for highly efficient electrophosphorescent devices. Adv Mater 2011;23:3876–3895.

[6] Tao YT, Yang CL, Qin JG. Organic host materials for phosphorescent organic light-emitting diodes. Chem Soc Rev 2011;40:2943–2970.

[7] Yasuda T, Shinohara Y, Matsuda T, Han LY, Ishi-i T. Improved power conversion efficiency of bulk-heterojunction organic solar cells using a benzothiadiazole–triphenylamine polymer. J Mater Chem 2012;22:2539–2544.

[8] Dutta P, Yang W, Eom SH, Lee SH. Synthesis and characterization of triphenylamine flanked thiazole-based small molecules for high performance solution processed organic solar cells. Org Electron 2012;13:273–282.

[9] Cai SY, Hu XH, Zhang ZY, Su JH, Li X, Islam A, Han LY, Tian H. Rigid triarylamine-based efficient DSSC sensitizers with high molar extinction coefficients. J Mater Chem A 2013;1:4763–4772.

[10] Singh SP, Roy MS, Thomas KRJ, Balaiah S, Bhanuprakash K, Sharma GD. New triphenylamine-based organic dyes with different numbers of anchoring groups for dye-sensitized solar cells. J Phys Chem C 2012;116:5941–5950.

[11] Metri N, Sallenave X, Plesse C, Beouch L, Aubert PH, Goubard F, Chevrot C, Sini G. Processable star-shaped molecules with triphenylamine core as hole-transporting materials: experimental and theoretical approach. J Phys Chem C 2012;116:3765−3772.

[12] Borsenberger PM, Weiss DS. Organic photoreceptors for xerography. New York: Marcel Dekker; 1998.

[13] Sato H, Hirai H, Son JM. Preparation of charge transporting polymers. J Synth Org Chem Jpn 2001;59:372−376.

[14] Yen HJ, Lin HY, Liou GS. Novel starburst triarylamine-containing electroactive aramids with highly stable electrochromism in near-infrared and visible light regions. Chem Mater 2011;23:1874–1882.

[15] Yen HJ, Liou GS. Novel blue and red electrochromic poly(azomethine ether)s based on electroactivettriphenylamine moieties. Org Electron 2010;11:299–310.

[16] Zhao ZJ, Li ZF, Lam JWY, Maldonado JL, Ramos-Ortiz G, Liu Y, Yuan WZ, Xu JB, Miao Q, Tang BZ. High hole mobility of 1,2-bis[4′-(diphenylamino)biphenyl-4-yl]-1,2-diphenylethene in field effect transistor. Chem Commun 2011;47:6924–6926.

[17] Yu XG, Yu JS, Zhou JL, Huang J, Jiang YD. Hole mobility enhancement of pentacene organic field-effect transistors using 4,4',4''-tris[3-methylphenyl(phenyl)amino] triphenylamine as a hole injection interlayer. Appl Phys Lett 2011;99:063306-1–063306-3.

[18] Wang B, Helander MG, Qiu J, Puzzo DP, Greiner MT, Hudson ZM, Wang S, Liu ZW, Lu ZH. Unlocking the full potential of organic light-emitting diodes on flexible plastic. Nature Photon 2011;5:753-757.

[19] Jin R, Tang S, Sun W. Rational design of donor–π–acceptor n-butyl-1,8-naphthalimide-cored branched molecules as charge transport and luminescent materials for organic light-emitting diodes. Tetrahedron 2014;70:47–53.

[20] Malinauskas T, Tomkute-Luksiene D, Daskeviciene M, Jankauskas V, Juska G, Gaidelis V, Arlauskas K, Getautis V. One small step in synthesis, a big leap in charge mobility: diphenylethenyl substituted triphenylamines. Chem Commun 2011;47:7770–7772.

[21] Zhan X, Risko C, Amy F, Chan C, Zhao W, Barlow S, Kahn A, Bredas J-L, Marder S.R. Electron affinities of 1,1-diaryl-2,3,4,5-tetraphenylsiloles: direct measurements and comparison with experimental and theoretical estimates. J Am Chem Soc 2005;127:9021–9029.

[22] Qiao Y, Wei Z, Risko C, Li H, Bredas J-L, Xu W, Zhu D. synthesis, experimental and theoretical characterization, and field-effect transistor properties of a new class of dibenzothiophene derivatives: from linear to cyclic architectures. J Mater Chem 2012;22:1313–1325.

[23] Kaafarani BR, El-Ballouli AO, Trattnig R, Fonari A, Sax S, Wex B, Risko C, Khnayze RS, Barlow S, Patra D, Timofeeva TV, List EJW, Bredas J-L, Marder SR. Bis(carbazolyl) derivatives of

pyrene and tetrahydropyrene: synthesis, structures, optical properties, electrochemistry, and electroluminescence. J Mater Chem C1 2013;1:1638–1650.

[24] Malinauskas T, Daskeviciene M, Kazlauskas K, Su HC, Grazulevicius JV, Jursenas S, Wu CC, Getautis V. Multifunctional red phosphorescent biscyclometallated iridium complexes based on 2-phenyl-1,2,3-benzotriazole ligand and carbazolyl moieties. Tetrahedron 2011;67:1852–1861.

[25] Lygaitis R, Grazulevicius JV, Gaidelis V, Jankauskas V, Sidaravicius J, Tokarski Z. 9-(4-Methoxyphenyl) carbazolyl-containing hydrazones for optoelectronic applications. Mol Cryst Liq Cryst 2005;427:407–418.

[26] Montrimas E, Gaidelis V, Pazera A. The discharge kinetics of negatively charged se electrophotographic layers. Lith J Phys 1966;6:569–576.

[27] Vaezi-Nejad SM. Xerographic time of flight experiment for the determination of drift mobility in high resitivity semiconductors. Int J Electron 1987;62:361–384.

[28] Stakhira P, Cherpak V, Volynyuk D, Ivastchyshyn F, Hotra Z, Tataryn V, Luka G. Characteristics of organic light emitting diodes with copper iodide as injection layer. Thin Solid Films 2010;518:7016-7018.

[29] Tsai MH, Hong YH, Chang CH, Su H-C, Wu CC, Matoliukstyte A, Simokaitiene J, Grigalevicius S, Grazulevicius JV, Hsu CP. 3-(9-carbazolyl)carbazoles and 3,6-di(9-carbazolyl)carbazoles as effective host materials for efficient blue organic electrophosphorescence. J Adv Mater 2007;19:862-866.

[30] Cherpak VV, Stakhira PY, Volynyuk DYu, Simokaitiene J, Tomkeviciene A, Grazulevicius JV, Bucinskas A, Yashchuk VM, Kukhta AV, Kukhta IN, et al. 3,6-Di(9-carbazolyl)-9-(2-ethylhexyl)carbazolebasedsingle-layer blue organic light emitting diodes. Synth Met 2011;161:1343-1346.

[31] Stakhira P, Khomyak S, Cherpak V, Volyniuk D, Simokaitiene J, Tomkeviciene A, Kukhta NA, Grazulevicius JV, Kukhta AV, Sun XW, et al. Blue organic light-emitting diodes based on pyrazolinephenyl derivative. Synth Met 2012;162:352–355.

[32] Volyniuk D, Cherpak V, Stakhira P, Minaev B, Baryshnikov G, Chapran M, Tomkeviciene A, Keruckas J, Grazulevicius JV. Highly efficient blue oleds based on intermolecular triplet-singlet energy transfer. J Phys Chem C 2013;117:22538−22544.

[33] Bushby RJ, McGill DR, Ng KM, Taylor N. p-Doped high spin polymers. J Mater Chem 1997;7(12):2343–2354.

[34] Vajiravelu S, Lygaitis R, Grazulevicius JV, Gaidelis V, Jankauskas V, Valiyaveettil S. Effect of substituents on the electron transport properties of bay substituted perylene diimide derivatives. J Mater Chem 2009;19:4268–4275.

[35] El-Khouly ME, Ju DK, Kay K-Y, D'Souza F, Fukuzumi S. Supramolecular tetrad of subphthalocyanine–triphenylamine–zinc porphyrin coordinated to fullerene as an "antenna-reaction-center" mimic: formation of a long-lived charge-separated state in nonpolar solvent. Chem Eur J 2010;16:6193–6202.

[36] Amthor S, Noller B, Lambert C. UV/Vis/NIR spectral properties of triarylamines and their corresponding radical cations. Chem Phys 2005;316:141–152.

[37] Frisch MJ, Trucks GW, Schlegel HB, Scuseria GE, Robb MA, Cheeseman JR, et al. Gaussian Inc. Wallingford CT;2009.

[38] Chen Y, Huang W, Li C, Bo Z. Synthesis of fully soluble azomethine-bridged ladder-type poly(p-phenylenes) by Bischler−Napieralski reaction. Macromolecules 2010;43:10216−10220

[39] Bushby RJ, Kilner CA, Taylor N, Vale ME. Disjoint and coextensive amminium radical cations: a general problem in making amminium radical cation based high-spin polymers. Tetrahedron 2007;63:11458–11466

[40] Brütting W, Berleb S, Mückl AG. Device physics of organic light-emitting diodes based on molecular materials. Org Electron 2011;2:1–36.

[41] Lee ST, Gao ZQ, Hung LS. Metal diffusion from electrodes in organic light-emitting diodes. Appl Phys Lett 1999;75:1404–1406.

TABLES

Table 1. Thermal characteristics of compounds **1**–**4**.

Compound	$T_{m.}$, ºC	T_g, ºC	T_{dec}, ºC
1	-	82	418
2	200	102	439
3	-	55	354
4	-	49	373

T_g estimated by DSC at heating rate of 10 ºC/min; N_2 atmosphere; second heating scan.

T_{dec} estimated by TGA at a heating rate of 20 ºC/min; N_2 atmosphere.

Table 2. Optical and photophysical characteristics of the dilute (10^{-5} M) solutions in THF and neat films of compounds **1**–**4**.

Compound	Solution							Film	
	in THF					in toluene			
	λ_{abs}^{max}, nm	λ_{F}^{max}, nm	Φ_F, %	τ, ns	χ^2	λ_{F}^{max}, nm	Φ_F, %	λ_{F}^{max}, nm	Φ_F, %
1	291, 395	511	12	0.57	1.256	488	14	497	3
2	286, 394	486	2	0.18	1.301	478	2	484	3
3	262, 358	469	30	1.51	1.127	444	33	466	2
4	272, 362	446	14	0.58	1.111	430	16	445	3

λ_{abs}^{max} – absorption maximum.

λ_{F}^{max} – emission maximum (λ_{ex} = 310 nm).

Φ_F – quantum yield.

τ – fluorescence life time measured at λ_{F}^{max} (λ_{ex} = 310 nm).

χ^2 – least squares fitting of experimental fluorescence decay data.

Table 3. I_p, EA, E_g energies and hole mobility data for compounds **1**–**4**.

Compound	$E_{1/2}$ vs Fc, V	E_g^{opt},[a] eV	I_p^{cv},[b] eV	EA^{cv},[c] eV	I_P^{ep},[d] eV	μ_0, cm^2/Vs	$\mu_{h,}$[e] cm^2/Vs
1	0.08	2.80	4.88	2.09	5.31	$2.6 \cdot 10^{-4}$	$4.2 \cdot 10^{-3}$
2	0.14	2.81	4.94	2.13	5.39	$7.1 \cdot 10^{-4}$	$7.9 \cdot 10^{-3}$
3	0.09	3.04	4.89	1.86	5.33	$1.6 \cdot 10^{-5}$	$6.5 \cdot 10^{-4}$
4	0.18	3.06	4.98	1.83	5.44	$3 \cdot 10^{-4}$	$5.8 \cdot 10^{-3}$

[a] The optical band gap estimated from the edges of electronic absorption spectra.

[b] The ionization potentials measured by electrochemical studies I_p^{cv}=4.8+$E_{1/2}$vsFc [21].

[c] The electron affinities calculated using equation $EA^{cv}= I_p^{cv} - E_g^{opt}$.

[d] The ionization potentials measured by electron photoemission in air method;

[e] Mobility value at $6.4 \cdot 10^5$ V/cm field strength.

FIGURES

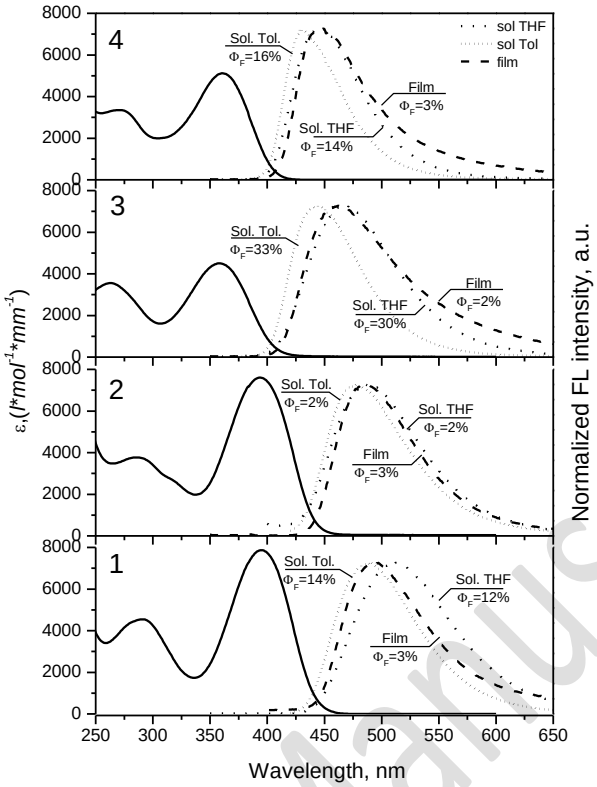

Figure 1. Absorption spectra of dilute (10^{-5} M) solutions in THF (solid lines) and fluorescence spectra of dilute solutions in THF and toluene and of the solid films of compounds **1-4** (λ_{ex} = 310 nm).

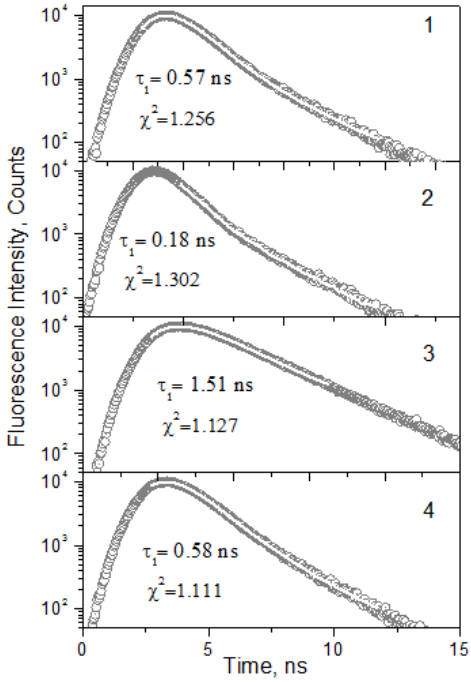

Figure 2. Fluorescence decay curves of dilute (10^{-5} M) solutions in THF (grey points) of compounds **1**–**4** (λ_{ex} = 310 nm). Lines mark exponential fits to the experimental data. Fluorescence lifetimes (τ) and least squares fitting of experimental data (χ^2) are indicated.

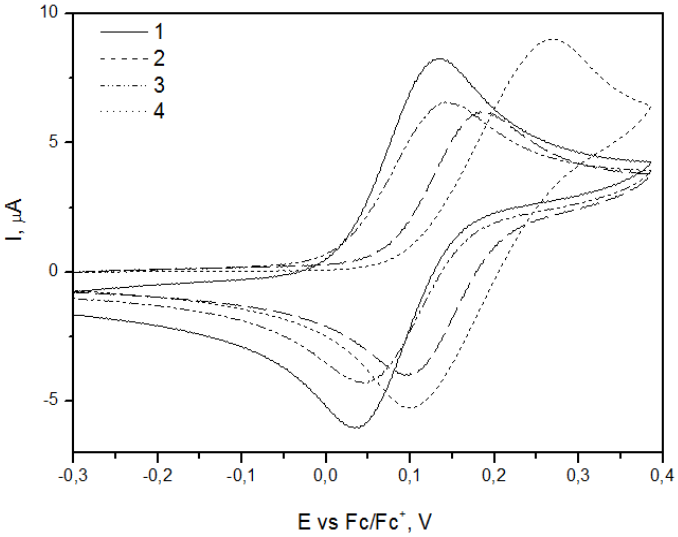

Figure 3. Cyclic voltammograms of dilute solutions of compounds **1**–**4** in dichloromethane recorded at 25 ^{o}C at the sweep rate of 0.1 V/s

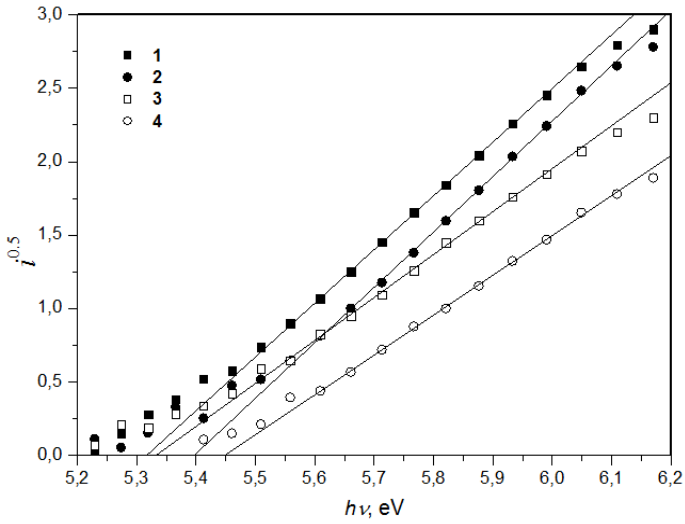

Figure 4. Electron photoemission spectra of the films of compounds **1**–**4** recorded in air at 25 °C.

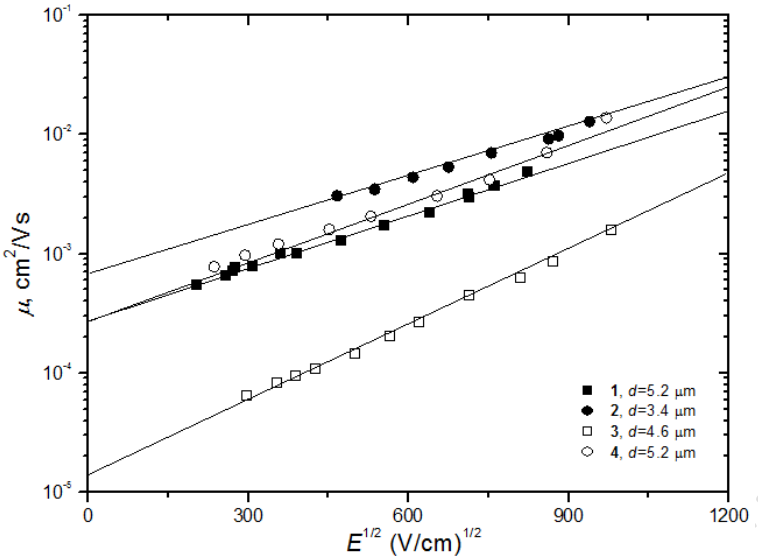

Figure 5. Electric field dependencies of hole drift mobilities for the layers of compounds **1**–**4**.

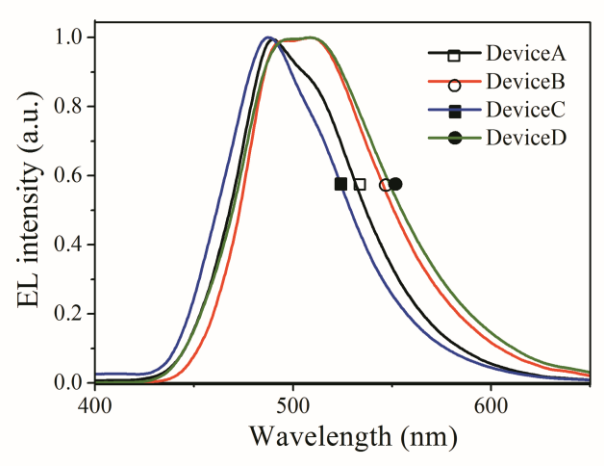

Figure 6. Electroluminescence spectra of OLEDs.

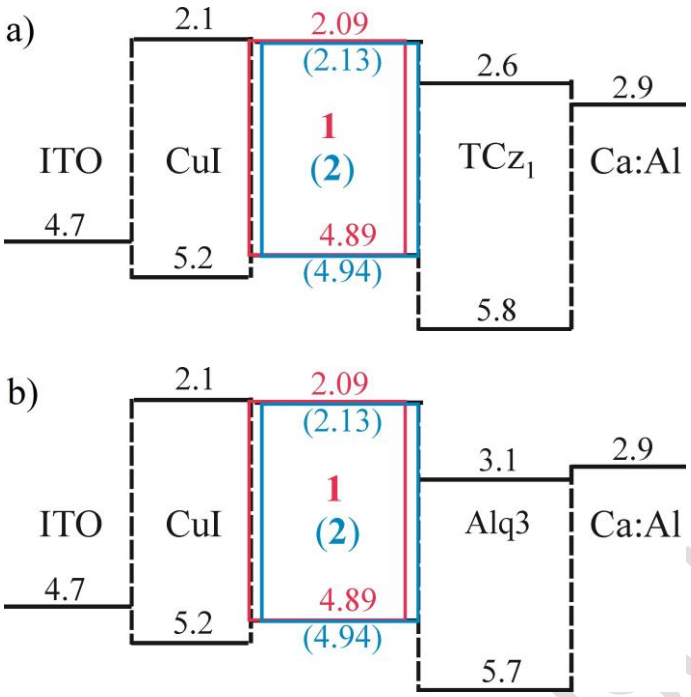

Figure 7. Energy-band diagrams of the devices A, C (a) and B, D (b).

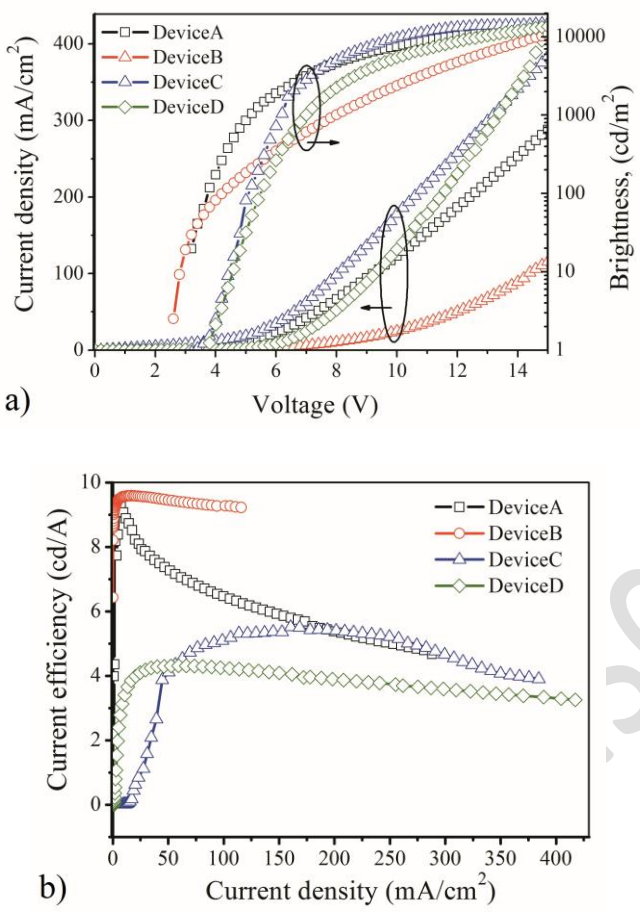

Figure 8. Current density-voltage and luminance-voltage characteristics (a) and current efficiency-current density characteristics (b) of OLEDs